

# Analog Coding of a Source with Erasures

Marina Haikin  
EE - Systems Department  
Tel Aviv University  
Tel Aviv, Israel  
Email: mkokotov@gmail.com

Ram Zamir  
EE - Systems Department  
Tel Aviv University  
Tel Aviv, Israel  
Email: zamir@eng.tau.ac.il

**Abstract**—Analog coding decouples the tasks of protecting against erasures and noise. For erasure correction, it creates an “analog redundancy” by means of band-limited discrete Fourier transform (DFT) interpolation, or more generally, by an over-complete expansion based on a frame. We examine the analog coding paradigm for the dual setup of a source with “erasure” side-information (SI) at the encoder. The excess rate of analog coding above the rate-distortion function (RDF) is associated with the energy of the inverse of submatrices of the frame, where each submatrix corresponds to a possible erasure pattern. We give a theoretical as well as numerical evidence that in each dimension where an equiangular tight frames (ETF) exists, it minimizes the excess rate over all possible frames. However, it does not achieve the RDF even in the limit as the dimension goes to infinity.

**Index Terms**—Data compression, side information, signal amplification, DFT, analog codes, frames, difference set, Welch bound, equiangular tight frames.

## I. INTRODUCTION

Consider a source sequence  $\mathbf{x}$  of  $n$  i.i.d samples from normal distribution  $\mathcal{N}(0, \sigma_x^2)$ . The encoder has information regarding the indices of  $k$  important samples. Denote by  $\mathbf{s}$  the vector of this side information. The decoder must reconstruct an  $n$ -dimensional vector  $\hat{\mathbf{x}}$  where only the values of samples dictated by  $\mathbf{s}$  matter, while at the non-important samples the distortion is zero:

$$D(x, \hat{x}, s) = \begin{cases} (\hat{x} - x)^2, & \text{if } s = 1 \text{ (important)} \\ 0, & \text{if } s = 0 \text{ (not important)} \end{cases} \quad (1)$$

In [1] it is shown that in this setting of erasure distortion, the encoder side information is sufficient, and the RDF is equal to that in the case where the side information is available to both the encoder and decoder:

$$R(D) = \frac{1}{2} \frac{k}{n} \log \left( \frac{\sigma_x^2}{D} \right), \quad (2)$$

where  $R$  is the rate per source sample,  $D$  is the average distortion at the important samples and  $\frac{k}{n}$  represents the probability of important samples. This rate can be achieved by an  $n$ -dimensional random code and joint-typicality encoding, with an *exponential* cost in complexity.

In this paper we explore the following “interpolate and quantize” analog coding scheme:

$$\mathbf{T}_{enc} \rightarrow Q \rightarrow \mathbf{T}_{dec} \quad (3)$$

and its achievable rate for different transforms  $\mathbf{T}_{enc}$  and  $\mathbf{T}_{dec}$ . Here,  $\mathbf{T}_{enc}$  is an  $n : m$  linear transformation that depends on  $\mathbf{s}$ ,  $\mathbf{T}_{dec}$  is an  $m : n$  linear transformation that is independent of  $\mathbf{s}$ , for some  $n \geq m \geq k$ , and  $Q(\cdot)$  denotes quantization. Typically we consider a constant ratio of important samples i.e  $k \approx n/2$  and are interested in the asymptotic performance ( $n \rightarrow \infty$ ).

One motivation for the analog coding scheme comes from a lossless compression version of this problem. In this setting, the encoder uses the Reed Solomon (RS) decoding algorithm to correct the erasures and determine the  $k$  information symbols. It then transmits these symbols to the decoder at a rate of  $\frac{k}{n} \log(J)$  bits per sample, where  $J$  is the size of the source alphabet. To reconstruct the source, the decoder uses the RS encoding algorithm to get the  $n$  reconstructed samples, that coincide with the source at the non-erased samples, as desired. we can view the RS decoder as a system which performs *interpolation* of the erased source signal.

Such an approach could be extended to a continuous source, if we first quantize the source to  $J$  levels and then apply the RS code solution above. However, this “quantize and interpolate” solution is limited to scalar quantization. Alternatively, the scheme in (3) reverses the order of quantization and interpolation and therefore it is not limited to scalar quantization. However, the interpolation step typically suffers from a *signal amplification* phenomenon. This is the main issue we deal with as it results in an increase in rate.

Our problem formulation is dual to Wolf’s paradigm of analog coding, in which transform techniques are exploited for channel coding with impulse noise [2]. Wolf’s scheme decouples impulse correction - by analog means - from additive white Gaussian noise (AWGN) protection - by digital means. The impulse-pattern dependent transform at the decoder introduces *noise amplification* for a general impulse pattern. In our case, the digital component is the quantizer, which is responsible for the lossy coding. The transform at the encoder causes signal amplification whose severeness depends on the pattern of important samples.

The main question which we explore is whether analog coding can asymptotically achieve the optimum information-theoretic solution. And even if not, what are the best transforms  $\mathbf{T}_{enc}$  and  $\mathbf{T}_{dec}$  in (3). Our preliminary results are unfortunately negative: the coding rate of the scheme in (3) is strictly above the RDF (2), even for the best transforms, and even if we let the dimension  $n$  go to infinity.

Several works explored frames which are good for other applications. In compressed sensing, for example, most commonly the goal is to maximize the spectral norm for all sub-matrices [3]. In [4], [5] frames for coding with erasures are introduced but they are tolerant only to specific patterns. In [6] ETFs are analyzed but only for small amount of erasures.

The main contributions introduced in this paper are the asymptotic point of view - concentration properties of ETFs and how they compare to random transforms, the redundant sampling ( $m > k$ ) approach, and the observation that ETFs are optimum in the sense of average signal amplification over all erasure

patterns. Section II describes the analog coding scheme in detail. Section III analyzes the performance of a random transform which is better than the basic DFT frame, while Section IV explores a superior approach of difference-set spectrum and general ETFs.

## II. SYSTEM CHARACTERIZATION

We begin with defining the system model. A *Transform Code* is characterized by a "universal" transform at the decoder and pattern dependent transform at the encoder. Let  $\mathbf{A}$  be the  $n \times m$  matrix representation of a frame with  $n$   $m$ -dimensional elements as rows, where  $\frac{m}{k} \triangleq \beta$  is the redundant-sampling ratio.<sup>1</sup>  $\mathbf{A}$  will serve as a transformation applied at the decoder, ( $\mathbf{T}_{dec}$  in (3)), independent of the pattern of important samples, as the side information is not available to the decoder. The pattern  $\mathbf{s}$  of the important samples defines which  $k$  rows of  $\mathbf{A}$  contribute to meaningful values. The corresponding rows construct the  $k \times m$  transform  $\mathbf{A}_s$ . Denote by  $\mathbf{B}_s$  the  $m \times k$  transform applied at the encoder, (nonzero part of  $\mathbf{T}_{enc}$  in (3)), to the vector  $\mathbf{x}_s$  of important samples.  $\mathbf{f} = \mathbf{B}_s \mathbf{x}_s$  is the vector of transformed samples. As illustrated in Figure 1, we use a white additive-noise model for the quantization of the  $m$  transformed samples, e.g. entropy coded dithered quantization (ECDQ), [7], which is blind to the locations of the important samples. As we recall, in the no-erasure case this additive-noise model can achieve the RDF with Gaussian noise (corresponding to large dimensional quantization) and Wiener filtering [8].

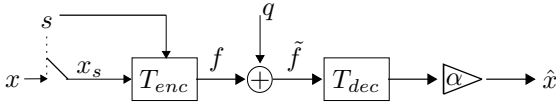


Fig. 1. Analog coding scheme.  $\mathbf{x}, \hat{\mathbf{x}}$  are  $n$ -dimensional vectors,  $\mathbf{x}_s$  is  $k$ -dimensional and  $\mathbf{f}, \tilde{\mathbf{f}}$  and  $\mathbf{q}$  are  $m$ -dimensional.

The  $k$  reconstructed important samples are thus

$$\hat{\mathbf{x}}_s = \alpha \mathbf{A}_s \tilde{\mathbf{f}} = \alpha \mathbf{A}_s (\mathbf{f} + \mathbf{q}) = \alpha \mathbf{A}_s \mathbf{B}_s \mathbf{x}_s + \alpha \mathbf{A}_s \mathbf{q} \quad (4)$$

where  $\tilde{\mathbf{f}}$  is the quantized version of the transformed samples and  $\mathbf{q}$  is a quantization noise with variance  $\sigma_q^2$ . We can deal separately with choice of  $\mathbf{B}_s$  and  $\alpha$ . The encoder applies  $\mathbf{B}_s$  such that  $\mathbf{A}_s \mathbf{B}_s = \mathbf{I}$  and  $\alpha$  is a Wiener coefficient.

Let  $\|\mathbf{A}_s\|^2$  denote the squared Frobenius norm of the matrix  $\mathbf{A}_s$  normalized by the number of the rows  $\|\mathbf{A}_s\|^2 = \frac{1}{k} \|\mathbf{A}_s\|_F^2 = \frac{1}{k} \sum_{i=1}^k \|\mathbf{A}_{s,i}\|^2$ , where  $\|\mathbf{A}_{s,i}\|$  is the  $l_2$  norm of  $i$ 'th row.

### A. Rate - Distortion Derivation

Since the decoder is blind to the transform, the rate is given by that of a white input with the same average variance [9]. The rate per sample for a pattern  $\mathbf{s}$  is therefore the mutual information in an AWGN channel with a white Gaussian input:

$$R = \frac{m}{n} \frac{1}{2} \log \left( 1 + \frac{\frac{1}{m} E \|\mathbf{f}\|^2}{\sigma_q^2} \right) \quad (5)$$

$$= \frac{m}{n} \frac{1}{2} \log \left( 1 + \frac{\sigma_x^2}{\sigma_q^2} \|\mathbf{B}_s\|^2 \right) \quad (6)$$

<sup>1</sup>This is unlike the conventions in frame theory in which the frame elements are column vectors.

where to obtain (6) we substitute the expression for the average variance of the transformed samples:

$$\frac{1}{m} E \|\mathbf{f}\|^2 = \frac{1}{m} \sum_{i=1}^m \sigma_{f_i}^2 = \frac{1}{m} \sum_{i=1}^m \|\mathbf{B}_{s,i}\|^2 \sigma_x^2 = \|\mathbf{B}_s\|^2 \sigma_x^2 \quad (7)$$

For a given  $\mathbf{A}_s$ , the  $\mathbf{B}_s$  that minimizes the expected  $l_2$  norm of  $\mathbf{f}$  in (5) is the pseudo-inverse  $\mathbf{B}_s = \mathbf{A}_s' (\mathbf{A}_s \mathbf{A}_s')^{-1}$ , hence<sup>2</sup>

$$\|\mathbf{B}_s\|^2 = \frac{1}{m} \|\mathbf{B}_s\|_F^2 = \frac{1}{m} \text{tr}(\mathbf{B}_s' \mathbf{B}_s) = \frac{1}{m} \text{tr}((\mathbf{A}_s \mathbf{A}_s')^{-1}) \quad (8)$$

We shall later see that the heart of the problem is the signal amplification caused by the factor  $\|\mathbf{B}_s\|^2$  in (6). If  $m = k$  then  $\mathbf{B}_s$  is uniquely given by  $\mathbf{A}_s^{-1}$ . The case of  $m > k$  is referred to as "redundant sampling", where more samples are quantized than the important ones. The motivation for this is the existence of more robust transforms in the sense of signal amplification even at the cost of some extra transmissions.

In order to preserve the distortion and avoid noise amplification, we restrict ourselves to transforms with unit norm of the rows,  $\|\mathbf{A}_{s,i}\| = 1$ : after the transformation at the decoder, the additive quantization noise at each sample has the variance  $\|\mathbf{A}_{s,i}\| \sigma_q^2 = \sigma_q^2$ . The variance of each sample of  $\mathbf{A}_s \mathbf{B}_s \mathbf{x}_s$  is  $\sigma_x^2$ . As a result of the Wiener estimation the distortion is:

$$D \triangleq E \left\{ \frac{1}{k} \sum_{i=1}^k D(x_i, \hat{x}_i, s_i) \right\} = \frac{1}{k} E \|\hat{\mathbf{x}}_s - \mathbf{x}_s\|^2 = \frac{\sigma_x^2 \sigma_q^2}{\sigma_x^2 + \sigma_q^2}. \quad (9)$$

Combining (6), (8) and (9) we can relate the rate and distortion of the scheme for a specific pattern  $\mathbf{s}$ :

$$R = \frac{m}{n} \frac{1}{2} \log \left( 1 + \frac{\frac{1}{m} \text{tr}((\mathbf{A}_s \mathbf{A}_s')^{-1}) (\sigma_x^2 - D)}{D} \right) \quad (10)$$

We define the excess rate of the scheme as  $\delta \triangleq R - R(D)$ :

$$\delta(\beta, \gamma, \eta_s) = \frac{k}{n} \frac{1}{2} [\beta \log(\eta_s \gamma + (1 - \eta_s)) - \log(\gamma)] \quad (11)$$

$$\simeq \rho_s + (\beta - 1) \frac{k}{n} \frac{1}{2} \log(\gamma) \quad (12)$$

where  $\gamma = \frac{\sigma_x^2}{D}$  is the signal-to-distortion ratio (SDR),

$$\eta_s = \frac{1}{m} \text{tr}((\mathbf{A}_s \mathbf{A}_s')^{-1}) \quad (13)$$

is the inverse energy (IE) of a pattern  $\mathbf{s}$ ,  $\rho_s = \frac{m}{n} \frac{1}{2} \log(\eta_s)$  and  $\simeq$  is true for high resolution ( $\gamma \gg 1$ ). We also define  $\rho$  as the mean logarithmic inverse energy (MLIE) of the frame  $\mathbf{A}$ :

$$\rho = \frac{1}{\binom{n}{k}} \sum_s \rho_s = \frac{1}{\binom{n}{k}} \sum_s \frac{m}{n} \frac{1}{2} \log(\eta_s) \quad (14)$$

i.e. the average (over all possible patterns of important samples) excess rate above the RDF caused by signal amplification. As we will see, asymptotically this average becomes the typical case.

In the high resolution case (12), the excess rate is composed of two elements, one as the result of the amplification and the second as a result of  $m - k$  extra samples transmission. Note that for fixed  $(n, k, \beta)$  minimizing the excess rate  $\delta$  is equivalent to minimizing the MLIE  $\rho$ .

<sup>2</sup> $(\ )'$  denotes the conjugate transpose.

## B. Side Information Transmission

It is required to compare the proposed system with the alternative naive approach of transmitting the side information regarding the locations of the important samples. Pattern transmission requires  $\frac{1}{n} \log \binom{n}{k}$  bits per input sample, which is  $H_b(k/n)$  bits in the limit  $n \rightarrow \infty$ .

## III. TRANSFORM OPTIMIZATION

### A. Band Limited Interpolation

The most basic frame includes  $m$  consecutive rows of the IDFT. Without loss of generality, the transform matrix  $\mathbf{A}$  consists of the first  $m$  columns of an IDFT matrix, meaning that the reconstructed samples are part of a band limited (lowpass) temporal signal with the quantized DFT coefficients as its spectrum ( $m$  lower frequencies). Such a transform  $\mathbf{A}$  forms a "full spark frame" - every subset of  $m$  rows of  $\mathbf{A}$  is independent, i.e.  $\mathbf{A}_s \mathbf{A}_s'$  is full rank and invertible for every pattern  $s$  [10]. However, it is not robust enough to different patterns. Though the source samples are i.i.d, the band limited model forces slow changes between close samples. Thus, it is good for uniform pattern, but for most other patterns it suffers from signal amplification that causes a severe loss in rate-distortion performance [7]. Asymptotically almost every sub-matrix  $\mathbf{A}_s$  is very ill-conditioned and the IE  $\eta_s$  (13) is unbounded even in case of redundant sampling  $\beta > 1$ .

### B. Signal Amplification

The following "Inversion-Amplification Lemma" describes the condition for optimal transform.

**Lemma 1:** The IE  $\eta_s$  in (13) of any  $k \times m$  matrix  $\mathbf{A}_s$ , s.t.  $\|\mathbf{A}_{s_i}\| = 1$ , is lower bounded as  $\eta_s \geq \frac{k}{m}$ , with equality iff  $\mathbf{A}_s \mathbf{A}_s' = \mathbf{I}$ .

*Proof:* Denote by  $\{\lambda_i\}_{i=1}^k$  the eigenvalues of  $\mathbf{A}_s \mathbf{A}_s'$ .

$$\begin{aligned} 1 &= \frac{1}{k} \text{tr}(\mathbf{A}_s \mathbf{A}_s') = \frac{1}{k} \sum_{i=1}^k \lambda_i \geq \frac{1}{\frac{1}{k} \sum_{i=1}^k \frac{1}{\lambda_i}} = \frac{1}{\frac{1}{k} \text{tr}((\mathbf{A}_s \mathbf{A}_s')^{-1})} \\ \Rightarrow \frac{1}{m} \text{tr}((\mathbf{A}_s \mathbf{A}_s')^{-1}) &= \frac{1}{\beta} \frac{1}{k} \text{tr}((\mathbf{A}_s \mathbf{A}_s')^{-1}) \geq \frac{1}{\beta}. \end{aligned}$$

where the inequality follows from the arithmetic-harmonic mean inequality, with equality iff all the eigenvalues have equal norm, i.e.  $\mathbf{A}_s \mathbf{A}_s' = \mathbf{I}$ . ■

For  $\beta = 1$ , Lemma 1 becomes  $\|\mathbf{A}_s^{-1}\| \geq 1$ , with equality iff  $\mathbf{A}_s$  is unitary. Thus for a non-unitary transform the signal is amplified by the factor  $\|\mathbf{A}_s^{-1}\|$ .

### C. Random Transforms

We know that random codes tend to be optimal. Thus, a natural approach is to understand what is the asymptotic performance of a random transform. Consider a matrix  $\mathbf{A}$  whose entries are i.i.d Gaussian random variables with variance  $\frac{1}{m}$ . For any  $k \times m$  sub-matrix  $\mathbf{A}_s$ ,  $\lim_{k \rightarrow \infty} \|\mathbf{A}_{s_i}\| = 1$  almost surely.

**1) Amplification Analysis:** We bring here two results which show that for  $m = k$ , random transform is definitely bad in the sense of amplification:

$$\lim_{k \rightarrow \infty} P\left[\frac{1}{k} \text{tr}((\mathbf{A}_s \mathbf{A}_s')^{-1}) \geq 1 + \zeta\right] = 1, \quad \forall \zeta \geq 0 \quad (15)$$

This means that with square random matrix we cannot achieve a 'non-amplifying' transformation. Moreover, w.p.1 the amplification diverges for large dimensions. For  $k \rightarrow \infty$  we can bound the divergence rate as follows:

$$\frac{k^2}{2\pi e} \leq E\left[\frac{1}{k} \text{tr}((\mathbf{A}_s \mathbf{A}_s')^{-1})\right] \leq \frac{k^3}{2\pi e} \quad (16)$$

The proof of both of these results is based on characterization of the minimum eigenvalue of a random matrix [11], and is omitted due to space constraints.

For  $m > k$  the amplification is finite. As random matrix theory shows, [11], if  $\mathbf{H}$  is an  $r \times t$  random matrix with i.i.d entries of variance  $\frac{1}{r}$  and  $\frac{t}{r} \rightarrow \beta, \beta > 1$ , then

$$\lim_{r \rightarrow \infty} \frac{1}{r} \text{tr}((\mathbf{H} \mathbf{H}')^{-1}) = \frac{1}{\beta - 1} \quad a.s. \quad (17)$$

A  $k \times m$  sub-matrix  $\mathbf{A}_s$  has element variance of  $\frac{1}{m}$ . Denote  $\mathbf{H} = \sqrt{\frac{m}{k}} \mathbf{A}_s$ , which has element variance of  $\frac{1}{k}$ :

$$\begin{aligned} \frac{1}{m} \text{tr}((\mathbf{A}_s \mathbf{A}_s')^{-1}) &= \frac{1}{k} \text{tr}((\mathbf{H} \mathbf{H}')^{-1}) \\ \Rightarrow \lim_{k \rightarrow \infty} \eta_s &= \frac{1}{\beta - 1}. \end{aligned} \quad (18)$$

**2) Comparison to the SI Transmission Benchmark (Section II-B):** Substituting (18) as the IE in (11) we get the following expression for the excess rate using a random transform:

$$\delta = \frac{k}{n} \frac{1}{2} \left[ \beta \log \left( \frac{1}{\beta - 1} \gamma + 1 - \frac{1}{\beta - 1} \right) - \log(\gamma) \right] \quad (19)$$

For some scenarios this outperforms the naive side information transmission.

Figure 2 shows the asymptotic excess rate above (2) for random transform with optimal  $\beta$  for each SDR compared to the cost of SI transmission.

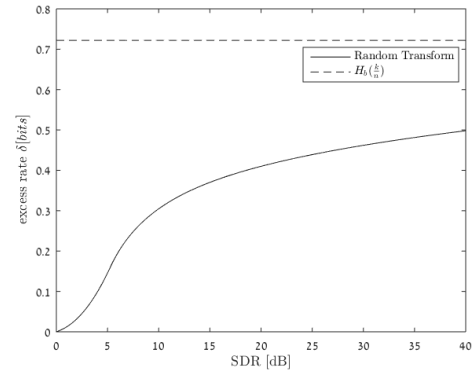


Fig. 2. Rate loss for  $\frac{k}{n} = \frac{1}{5}$ .

In the limit of high SDR the expression for the excess rate (for the best choice of  $\beta$ ) takes the following form:

$$\delta = \frac{k}{n} \frac{1}{2} \log(\ln(\gamma)), \quad (20)$$

which goes (very slowly) to  $\infty$ . Nevertheless, for reasonably high SDR there is advantage to random matrix approach relative to the benchmark. Analysis of  $\beta$  which minimizes the rate loss in (19) and the proof of (20) are omitted here due to space limitations.

#### IV. IRREGULAR SPECTRUM

In this section we show empirically, as well as give theoretical evidence, that a scheme based on an *irregular spectrum* or an ETF beats the naive benchmark (Section II-B) and also the random matrix approach (Section III-C) in the sense of achievable rate.

##### A. Model Selection and Motivation

When constructing a transform based on the IDFT matrix, the guiding idea is to be more robust to different patterns of important samples than the band limited interpolation frame of Section III-A. A better approach would be to select an irregular ‘symmetry breaking’ set of frequencies. Thus, the encoder performs interpolation to a signal with irregular spectrum. Every choice of frequency pattern forms a frame  $\mathbf{A}$ , which consists of the columns of the IDFT matrix that correspond to the frequency pattern.

For general spectral pattern the corresponding frame is not necessarily full spark (for a general  $n$ ). But for prime  $n$ , Chebotarev’s theorem guarantees that for every spectral choice and every pattern of important samples,  $\mathbf{A}_s^{-1}$  (or the pseudo inverse) exists [12]. We thus restrict the discussion to prime  $ns$  when exploring the DFT transform.

##### B. Difference Set Spectrum

For small dimensions it is possible to exhaustively check all spectrum choices and look for the one with the best worst case or average amplification ( $\rho_s$ ). It turns out that the best spectrum consists of frequencies from a *difference set* (DS), forming the so called difference-set spectrum (DSS).

*Definition:* an  $m$  subset of  $\mathbb{Z}_n$  is a  $(n, m, \lambda)$  difference set if the distances (modulo  $n$ ) of all distinct pairs of elements take all possible values  $1, 2, \dots, n-1$  exactly  $\lambda$  times. The three parameters must satisfy the relation

$$\lambda(n-1) = m(m-1). \quad (21)$$

Difference sets are known to exist for some pairs of  $(n, m)$ . We consider the case of prime  $n$  and  $m \approx \frac{n}{2}$ . Specifically, we consider a *Quadratic Difference Set* [13] with the following parameters:

$$\left( n = p, m = \frac{p-1}{2}, \lambda = \frac{p-3}{4} \right), \quad p - \text{prime}. \quad (22)$$

This DS can be constructed by a cyclic sub group  $\langle g \rangle$ , for some element  $g$  from the multiplicative group of  $\mathbb{Z}_n$ .

Figure 3 shows the histogram of  $\eta_s$  over randomly chosen patterns for a large dimension in the case of a random transform and a DSS transform. We see that the IE of a random transform concentrates on  $\frac{1}{\beta-1}$  (18). Interestingly, also for DSS almost all patterns (sub-matrices) are equivalent and the IE concentrates on a lower value. The ideal lower bound (of Lemma 1) is also presented (along the y axis). The advantage of the DSS lies in its better eigenvalue distribution.

Recall that the IE is determined by the eigenvalues distribution (Lemma 1). Figure 4 shows the empirical distribution of the eigenvalues of  $\mathbf{A}_s \mathbf{A}_s'$  for different transforms. Figure 4 shows also the theoretical limiting eigenvalue density of a random matrix [11]. Observe the concentration property of the eigenvalues empirical distribution and of the IE  $\eta_s$  (13), namely with high probability these random functionals are close to their mean value. Observe also that the minimal eigenvalue of a random transform is closer to zero and thus its contribution to the IE amplification

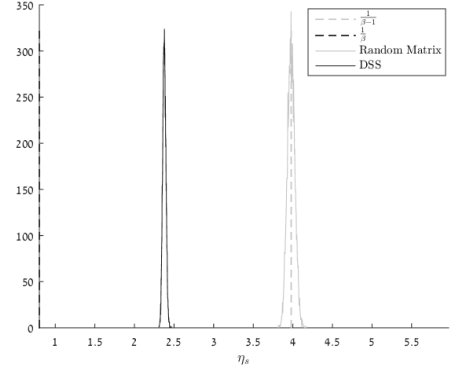


Fig. 3. Histogram of the inverse energy  $\eta_s$  for  $n = 947, \beta = 1.25$ .

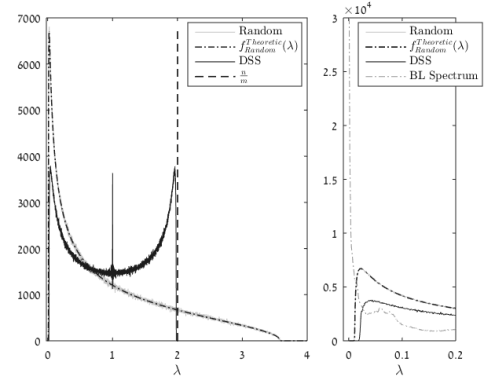


Fig. 4. Eigenvalue distribution of  $\mathbf{A}_s \mathbf{A}_s'$ ,  $n = 947, \beta = 1.25$ . The graph on the right hand side zooms in into the behavior near zero.

is more significant. As  $\beta$  decreases, the extremal eigenvalues move towards the edges (0 and  $\frac{n}{m}$ ), and the minimal eigenvalue becomes the most dominant for the IE. For  $\beta = 1$ , the density function is very high around zero and as a result the IE diverges and there is no concentration to finite value. Note that in band limited interpolation this is the case even for  $\beta > 1$ .

Interestingly, asymptotically in this setup a random spectrum achieves similar performance as the DSS.

##### C. Equiangular Tight Frames

It turns out that DSS spectrum forms an *equiangular tight frame* (ETF) or *maximum-Welch-boud-equality codebook* (MWBE) [13]. Moreover, we observe that asymptotically many different ETFs are similar in terms of  $\rho_s$  distribution and this indicates that the strength of irregular spectrum lies in its properties as an ETF.

An  $n \times m$  transform  $\mathbf{A}$  is constructed from the  $m$  columns of  $n \times n$  IDFT matrix that correspond to indices from a difference set. The normalization of the IDFT is such that  $\|\mathbf{A}_i\| = 1$ , i.e the absolute value of the elements is  $\frac{1}{\sqrt{m}}$ . According to the tightness and the equiangularity definitions, the properties of this construction are:  $\mathbf{A}'\mathbf{A} = \frac{n}{m}\mathbf{I}_m$ , and the absolute value of the correlation between two rows is constant for all pairs and is equal to the Welch bound:

$$|\mathbf{a}_l \mathbf{a}_{l'}'| = \sqrt{\frac{n-m}{(n-1)m}} = \cos(\theta), \quad \forall l \neq l'. \quad (23)$$

The matrix  $\mathbf{A}\mathbf{A}'$  is Hermitian positive semidefinite whose diagonal elements are 1 and whose off-diagonal elements have equal

absolute value  $\cos(\theta)$  as in (23). It has  $m$  eigenvalues equal to  $\frac{n}{m}$  (same as in  $\mathbf{A}'\mathbf{A}$ ) and the rest  $n - m$  eigenvalues are zero. For any  $k \leq m$  rows of  $\mathbf{A}$  (induced by the important samples pattern  $s$ )  $\mathbf{A}_s\mathbf{A}_s'$  is positive definite. The structure of the  $k \times k$  matrix  $[\mathbf{A}_s\mathbf{A}_s']$  is the same as that of the  $n \times n$  matrix  $[\mathbf{A}\mathbf{A}']$ , up to different dimension, but the phases of the off-diagonal elements "behave" differently. As a result, the eigenvalue spectrum of  $\mathbf{A}_s\mathbf{A}_s'$  is none of the same. The distribution of this spectrum is the main issue of interest when exploring the IE  $\eta_s$  (Figure 4).

**Lemma 2:** Let  $\mathbf{A}$  be a DSS frame matrix whose frequencies correspond to the difference set (22). Then the off-diagonal elements of  $\mathbf{A}\mathbf{A}'$  consist of two values  $\cos(\theta)e^{j\phi}$  or  $\cos(\theta)e^{-j\phi}$ . Asymptotically,  $\phi \rightarrow \frac{\pi}{2}$  as  $n \rightarrow \infty$ , so the off-diagonal elements are  $\pm i\sqrt{\frac{n-m}{(n-1)m}}$ .

This result is interesting as many other families of ETFs (based on conference matrices) exist for which the correlation values are  $\pm i\cos(\theta)$  (or  $\pm\cos(\theta)$  for real frames) not only asymptotically. Every type exist for different pairs of  $n$  and  $m \approx \frac{n}{2}$  [14],[15].

The IE of a submatrix of an ETF satisfies the following lower bound.

**Lemma 3:** If  $\mathbf{A}$  is an ETF, then for  $\beta = 1$ ,  $\eta_s \geq \sin^{\frac{2(1-k)}{k}}(\theta)$  for every submatrix  $\mathbf{A}_s$ .

Unfortunately, this lower bound is asymptotically trivial and coincides with Lemma 1 as  $\eta_s \geq 1$ . The proofs of the two Lemmas above are omitted due to space constraints.

While DFT based transforms assume a complex source, ETFs allow us to consider real valued sources which is our original motivation. As stated before, other types of ETFs mentioned above achieve similar IE distribution. Figure 5 shows the histogram of  $\delta$ , as defined in (12), for random transform and Paley's real ETF [16], for particular value of high SDR.

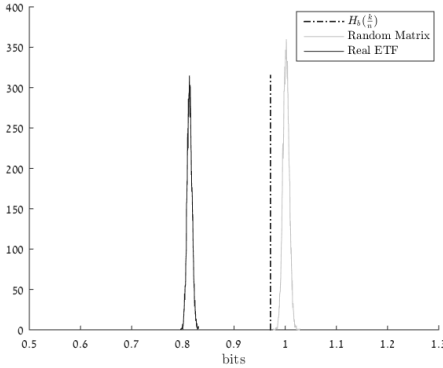


Fig. 5. Histogram of  $\delta$ ,  $n = 948$ ,  $m = \frac{n}{2}$ ,  $\beta = 1.25$ ,  $\text{SDR} = 30\text{dB}$ .

We can see that for this setup the random transform is a bit worse than SI transmission, but a scheme based on a real-valued ETF achieves a lower rate.

Finally, We have a strong evidence that ETFs are optimal in the sense of average excess rate caused by signal amplification, i.e achieve the least MLIE defined in (14) over all possible  $(n, m)$  frames. Here we develop a simplified version of this conjecture, stating that the ETF is a local minimum, i.e the gradient of the MLIE with respect to all elements of  $\mathbf{A}$  is zero at an ETF. The minimization is constrained due to the unit norm row constraint. Thus, the following term is added to the Lagrangian:  $L = \rho + \sum_{u=1}^n \lambda_u (\sum_{v=1}^m |\mathbf{A}_{u,v}|^2 - 1)$ . The elements of  $\rho$  which

depend on  $\mathbf{A}_{i,j}$  are those for which  $s$  includes sample  $i$  in the pattern of important samples. Such patterns produce  $\mathbf{A}_{s^i}$  which consists of row  $i$  and  $\binom{n-1}{k-1}$  other rows of  $\mathbf{A}$ . Denote by  $r_{s^i}$  the location of row  $i$  with respect to  $k$  rows corresponding to pattern  $s^i$ . We use the following matrix derivative result:  $\frac{\partial}{\partial \mathbf{X}} \text{tr}(\mathbf{X}^{-1}) = -(\mathbf{X}^{-2})^T$ . The derivative of  $L$  with respect to  $\mathbf{A}_{i,j}$ ,  $\frac{\partial}{\partial \mathbf{A}_{i,j}} L$  is:

$$\frac{1}{\binom{n}{k}} \frac{1}{n \ln(2)} \sum_{s^i=1}^{\binom{n-1}{k-1}} \sum_{t=1}^k \frac{(\mathbf{A}_{s^i} \mathbf{A}_{s^i}')^{-2}_{r_{s^i}, t} (\mathbf{A}_{s^i})_{t, j}}{\frac{1}{m} \text{tr}((\mathbf{A}_{s^i} \mathbf{A}_{s^i}')^{-1})} - 2\lambda_i \mathbf{A}_{i, j} \quad (24)$$

Note that for simplicity we assumed here real frame, but the result is true also for complex frames. Numerically, substituting different normalized ETFs for various dimensions  $\frac{\partial}{\partial \mathbf{A}_{i,j}} L$  is zeroed for all  $i, j$ . Specifically, this was verified for complex DSS and real ETF based on Paley's construction of symmetric conference matrices [16].

## V. CONCLUDING REMARKS

Our results indicate that analog coding with "good" frames outperforms both band-limited interpolation and random frames, but it is inferior to the pure digital (rate-distortion function achieving) solution. DSS frames, and more generally - ETFs - seem to be the natural candidates for optimal analog-coding frames. Furthermore, this family of frames seem to exhibit a limiting behavior as the dimension goes to infinity. Although the question of whether they are indeed optimal remains open, our current results strongly support a positive answer.

## REFERENCES

- [1] E. Martinian, G. Wornell, and R. Zamir, "Source coding with distortion side information," *IEEE Trans. Inf. Theory*, vol. 54, no. 28, pp. 4638–4665, Oct. 2008.
- [2] J.K. Wolf, "Redundancy, the Discrete Fourier Transform, and Impulse Noise Cancellation," *IEEE Trans. on Communications*, vol. 31, no. 3, pp. 458–461, March 1983.
- [3] E.J. Candès, "The restricted isometry property and its implications for compressed sensing," *C. R. Math.*, vol. 346, no. 9, pp. 589–592, May 2008.
- [4] G. Rath and C. Guillemot, "Frame-theoretic analysis of DFT codes with erasures," *IEEE Trans. Signal Process.*, vol. 52, no. 2, pp. 447–460, Feb. 2004.
- [5] M. Vaezi and F. Labeau, "Systematic DFT frames: principle, eigenvalues structure, and applications," *IEEE Trans. Signal Process.*, vol. 61, no. 15, pp. 3774–3885, Aug. 2013.
- [6] R. Holmes, V. Paulsen, "Optimal frames for erasures," *Linear Algebra Appl.*, vol. 377, pp. 31–51, 2004.
- [7] A. Mashiah, and R. Zamir, "Noise-shaped quantization for nonuniform sampling," in *Proc. Int. Symp. Info. Theory*, pp. 1187–1191, Jul 2013.
- [8] T. Berger *Rate Distortion Theory: A Mathematical Basis for Data Compression*. Prentice Hall, 1971.
- [9] A. Lapidoth, "On the role of mismatch in rate distortion theory," *IEEE Trans. Inf. Theory*, vol. 43, no. 1, pp. 38–47, Jan. 1997.
- [10] Alexeev, J. Cahill, and D.G. Mixon, "Full Spark Frames," *J. Fourier Anal. Appl.*, vol. 18, pp. 1167–1194, 2012.
- [11] A. M. Tulino and S. Verdú, *Random Matrix Theory and Wireless Communications*. now Publishers, 2004.
- [12] Steinhagen, P., Lenstra, H.W.: "Chebotarëv and his density theorem," *Math. Intelligencer*, vol. 18, pp. 26–37, 1996.
- [13] P. Xia, S. Zhou, and G. B. Giannakis, "Achieving the Welch bound with difference sets," *IEEE Trans. Inform. Theory*, vol. 51, no. 5, pp. 1900–1907, May 2005.
- [14] M.A. Sustik, J.A. Tropp, I.S. Dhillon, R.W. Heath Jr., "On the existence of equiangular tight frames," *Appl. Comput. Harmon. Anal.*, vol. 426, pp. 619–635, 2007.
- [15] T. Strohmer and R. W. Heath Jr., "Grassmannian frames with applications to coding and communication," *Appl. Comput. Harmonic Anal.*, vol. 14, no. 3, pp. 257–275, 2003.
- [16] R.E.A.C. Paley, "On orthogonal matrices," *J. Math. Phys.*, vol. 12, pp. 311–320, 1933.